Journal of the European Ceramic Society 21 (2001) 2577–2582

www.elsevier.com/locate/jeurceramsoc

Self-diffusion of oxygen in mullite

P. Fielitz[a,*], G. Borchardt[a], H. Schneider[b], M. Schmücker[b], M. Wiedenbeck[c], D. Rhede[c]

[a]FB Physik, Metallurgie und Werkstoffwissenschaften, Technische Universität Clausthal, Institut für Metallurgie, Robert-Koch-Str. 42, Clausthal, Germany
[b]Institut für Werkstoff-Forschung, Deutsches Zentrum für Luft- und Raumfahrt, Porz-Wahnheide, Linder Höhe, D-51147 Köln, Germany
[c]GeoForschungsZentrum Potsdam, Telegrafenberg, D-14473 Potsdam, Germany

Abstract

The mullite structure is a model silicate system from the point of view of (geo-)materials science. Available oxygen diffusivity data for 3/2 and 2/1 (alumina/silica) mullite single crystals are jointly discussed together with the oxygen diffusion data in other generic oxides in terms of empirical correlations. Oxygen vacancies are identified as the majority defects responsible for oxygen transport in both mullite materials.

Keywords: Diffusion; Mullite

1. Introduction

Quantitative information of the atomic mobilities of the constituent elements, as a function of the pertinent thermodynamic potentials, is needed in order to explain diffusion controlled solid state transport phenomena occurring in earth sciences and in materials science, e.g. creep, solid state reactions and some phase transformations. As to silica based minerals and materials, the situation is characterised by the lack of suitable radioactive tracers for the major constituents silicon and oxygen (this is also true for magnesium and aluminium). The available data are, therefore, based on stable isotope work and, in a few cases, on interdiffusion experiments (e.g. for silicon or aluminium). In this paper we focus on the oxygen sublattice of mullite. Available oxygen diffusion data on other close packed oxides and on mullite will be jointly correlated through semi-quantitative relations. The mullite data will be further rationalised through a point defect approach.

2. Experimental data on oxygen diffusion in mullite

Mullite $Al_2[Al_{2+2x}Si_{2-2x}]O_{10-x}$ is a non-stoichiometric phase with x denoting the number of oxygen vacancies per unit cell. The mullite structure consists of chains of edge-sharing AlO_6 octahedra running parallel to the crystallographic c-axis. These octahedra chains are cross-linked by $(Al,Si)O_4$ tetrahedra forming double chains, which also run parallel c (Fig. 1).

The symmetry of the average structure belongs to the space group Pbam. The compositional variation in mullite results from substitution of Si^{4+} by Al^{3+} and a simultaneous formation of oxygen vacancies according to the Kröger-Vink notation:

$$Al_2O_3 + 2\ Si_{Si} + O_o \Longleftrightarrow 2\ Al'_{Si} + V^{\cdot\cdot}_o + 2\ SiO_2 \qquad (1)$$

To date little knowledge on the diffusion in mullite single crystals is available. Studies on the iron incorporation and associated 2/1- to 3/2-mullite phase transformation actually yielded stronger penetration depths along c than perpendicular to it.[1] This was interpreted in terms of faster diffusion of iron along c rather than perpendicular to c. Recently, ^{18}O tracer diffusion in 3/2-mullite was indirectly observed on micrometer size single crystals by measuring the concentration of ^{18}O in the gaseous phase:[2]

$$D_{3/2} = (1.32 \pm 0.39) \times 10^{-6}\frac{m^2}{s}\exp\left(-\frac{(397 \pm 45)kJ/mol}{RT}\right) \qquad (2)$$
$$\text{for} \quad 1373\ K \leqslant T \leqslant 1573\ K$$

The most direct way to measure mobility differences along the crystallographic axes is SIMS depth profiling of isotopes. For details of our own ^{18}O isotope exchange experiments on single crystalline 2/1-mullite samples

* Corresponding author. Tel.: +49-5323-72-2634; fax: +49-5323-72-3184.
E-mail address: peter.fielitz@tu-clausthal.de (P. Fielitz).

0955-2219/01/$ - see front matter
PII: S0955-2219(01)00276-X

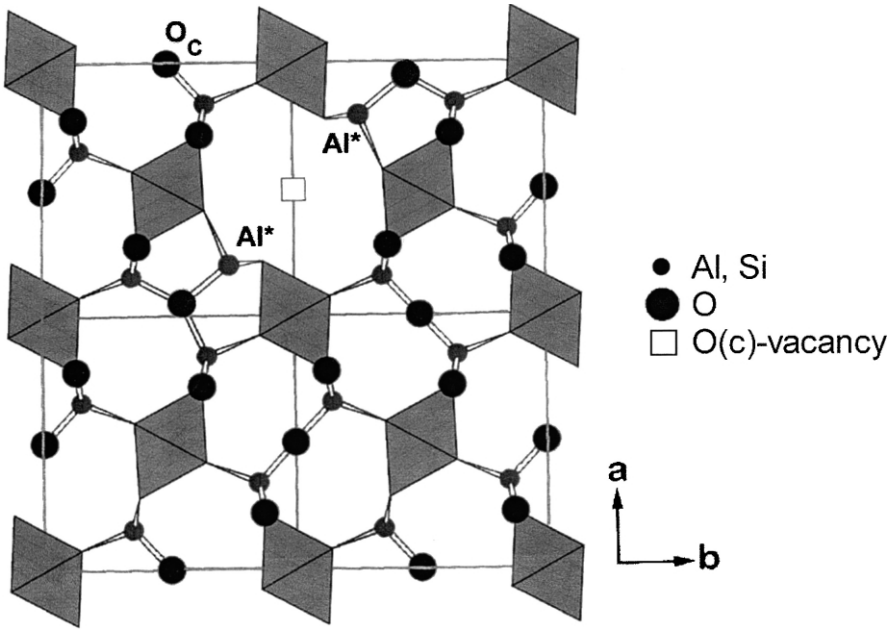

Fig. 1. Crystal structure of mullite in projection along the c-axis.

parallel to the crystallographic *b*- and *c*-axis we refer to our recent work.[3] The slight anisotropy observed was in the estimated error range (±30%) of our diffusion data, which is typical for SIMS depth profiling. A linear fit of the temperature dependence results in the following Arrhenius relation for the oxygen diffusion in 2/1-mullite:

$$D_{2/1} = \left(3.71^{+13}_{-3}\right) \times 10^{-5} \frac{\mathrm{m}^2}{\mathrm{s}} \exp\left(-\frac{(433 \pm 21)\mathrm{kJ/mol}}{RT}\right) \quad \text{for } 1523\ \mathrm{K} \leqslant T \leqslant 1798\ \mathrm{K} \tag{3}$$

3. Correlation of oxygen diffusivities in close packed oxides

3.1. Estimation of oxygen diffusivities by an empirical relation after Reddy and Cooper

Reddy and Cooper[4] found that in close packed oxides there is a good correlation between the oxygen diffusivity and the oxygen density and the melting temperature of a given oxide. Examination of the activation enthalpies h_{act} and corresponding oxygen densities (i.e. the number of oxygen atoms per unit volume, ρ_o) indicated that the ratio h_{act}/ρ_o^2 is virtually constant (see Table 1).

A correlation between the defect activation enthalpy and the oxygen density is understandable because an increase in oxygen density means closer packing of oxygen and therefore greater difficulty for the oxygen atoms to move. The reason why h_{act} is proportional to ρ_o^2 instead of ρ_o is not clear. The transformation given below projects all measured diffusion data into one Arrhenius plot for $D_{oxygen} = D_{oxygen}(T^*(\Delta\rho_o,\ \Delta T_m))$ by moving the individual straight lines proportionally to the oxygen density difference and the difference in melting temperature ΔT_m, i.e.

$$\frac{1}{T^*} = \frac{\rho_o^2}{T} + C_1\Delta\rho_o + C_2\Delta T_m \qquad \begin{matrix} C_1 = -4.7 \times 10^{-4}; \\ C_2 = -2.5 \times 10^{-8}; \end{matrix}$$

$$\Delta\rho_o = \rho_o - 0.535$$

$$\Delta T_m = 3123 - T_m$$

$$D_{oxygen} = 3.0 \times 10^{-10} \frac{m^2}{s} \exp\left(-\frac{1.3 \times 10^5}{T^*}\right) \tag{4}$$

$$\rho_o = \left(\text{number of oxygen ions/m}^3\right) \times 10^{-29};$$

$$T_m = \text{melting temperature/K}$$

The resulting master curve is shown in Fig. 2. This empirical correlation is useful in order to estimate the oxygen diffusivity in close packed oxides if there are no experimental data available. Using the melting temperature $T_m = 1890°C$ and the oxygen density $\rho_o = 0.571 \times 10^{29}$ m^{-3} for 2/1-mullite[5] one gets the dotted line shown in Fig. 3 together with the only published experimental data.[2,3]

3.2. Compensation rule for oxygen self-diffusion in close packed oxides

The compensation "law" or isokinetic effect[6] is an empirical linear correlation between the logarithm of the pre-exponential factor D_0 and the defect activation enthalpy h_{act}:

$$\ln(D_0) = m_1 \cdot h_{act} + \ln\left(D_1^*\right) \quad \text{in the interval } [T_{min}, T_{max}] \tag{5}$$

Table 1
Comparison of oxygen diffusion data, melting temperature and oxygen density in close packed oxides[4]

Mineral	D_0 (m^2/s)	h_{act} (kJ/mol)	Melting temperature T_m (K)	Oxygen density ρ_o ($10^{29}/m^3$)	h_{act}/ρ_o^2 ($\delta\ 10^{-58}$ kJ m^6/mol)	Range T_{min} (K)	Range T_{max} (K)
Al_2O_3 (hexagonal)	2.7×10^{-02}	615	2323	0.703	1244	1723	1948
$MgAl_2O_4$ (cubic)	1.0×10^{-06}	410	2408	0.610	1102	1623	1923
Mg_2SiO_4 (distorted hexagonal)	3.5×10^{-07}	372	2183	0.550	1230	1573	1873
MgO (cubic)	2.0×10^{-08}	370	3123	0.535	1296	1623	1823

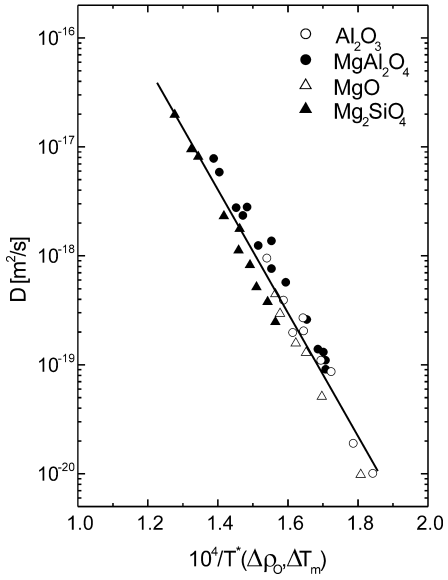

Fig. 2. Master curve for oxygen diffusivities in close packed oxides (after Reddy and Cooper).[4]

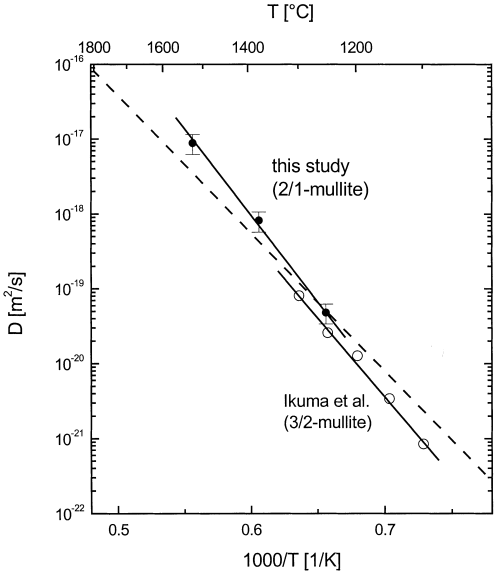

Fig. 3. Oxygen diffusivities in mullite. Full points: experimental data, our work;[3] open points, Ikuma et al.;[2] dotted line: oxygen diffusivity estimated with the Reddy–Cooper relation [Eq. (4)].

where m_1 is the slope and D_1* the pre-exponential factor for $h_{act}=0$. This correlation can only be checked in the interval $[T_{min}, T_{max}]$ that is given by the accessible temperature range of the diffusion measurements (see Table 1). It was first assessed for metals by Zener.[8] Recently, Jaoul and co-workers gave an analogous interpretation of silicon tracer diffusion data in some closely related silicate structures.[9]

On the other hand, for self-diffusion the following equation is valid:[7]

$$D = \Gamma\ \exp\left(-\frac{g_{act}}{RT}\right) = \Gamma\ \exp\left(\frac{s_{act}}{R}\right)\exp\left(-\frac{h_{act}}{RT}\right) = D_0\ \exp\left(-\frac{h_{act}}{RT}\right) \quad (6)$$

where Γ is virtually temperature and pressure independent. In a cubic structure, Γ can be calculated by $\Gamma = fa^2\nu$, where f is a correlation factor, a is the lattice parameter and ν the vibration frequency ($\approx$ the Debye frequency). The free enthalpy of activation, and the activation entropy are denoted by g_{act} and s_{act}, respectively. From Eq. (6) one gets:

$$\ln(D_0) = \frac{s_{act}}{R} + \ln\Gamma \quad (7)$$

Comparing Eqs. (5) and (7), one finds:

$$h_{act} = T^* s_{act} + RT^* \ln\frac{\Gamma}{D_1^*} \quad \text{with} \quad T^* \equiv \frac{1}{m_1 R} \quad \text{in the interval } [T_{min}, T_{max}] \quad (8)$$

This means that there is a linear correlation between activation enthalpy and entropy if the compensation law exists. The temperature T * is called "isokinetic" temperature[6] because at T * all diffusivities are equal to D_1* [which is easy to check by inserting Eq. (8) into (6)].

If we try to verify the compensation law in a [log (D_0), h_{act}] diagram for various close packed oxides we get a fairly big scatter for a linear plot (Fig. 4). But if the melting temperatures (also shown in Fig. 4) are also

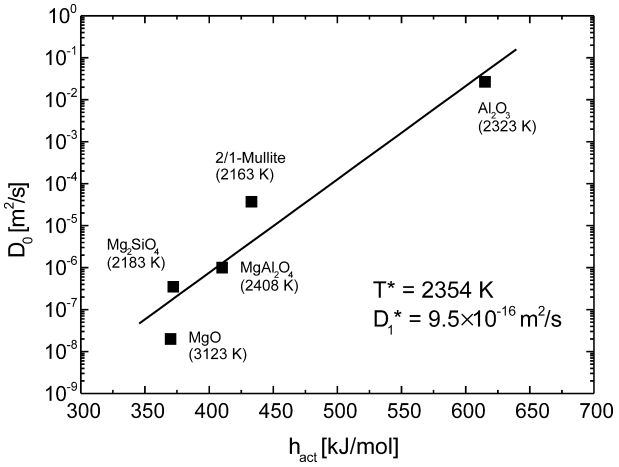

Fig. 4. Check of the compensation law for oxygen diffusion in different close packed oxides (data see Table 1). A linear fit results in the isokinetic temperature T^* and the isokinetic diffusion coefficient D_1^*. The temperatures in brackets are the melting temperatures of the oxides.

taken into consideration a correlation between the melting temperature T_m and the isokinetic temperature T^* becomes obvious. In other words: there exists no universal (isokinetic) temperature for all the different close, packed oxides, and only close packed oxides with a similar melting temperature seem to show a good correlation in a [log (D_0), h_{act}] diagram.

Fig. 5, therefore, suggests the relation $T^* = \gamma T_m$ which gives the following linear correlations in the interval [T_{min}, T_{max}]:

$$\ln(D_0) = m_2 \cdot \frac{h_{act}}{T_m} + \ln\left(D_2^*\right) \tag{9}$$

$$\frac{h_{act}}{T_m} = \gamma s_{act} + R\gamma \ln\frac{\Gamma}{D_2^*} \quad \text{with} \quad \gamma = \frac{1}{m_2 R} \tag{10}$$

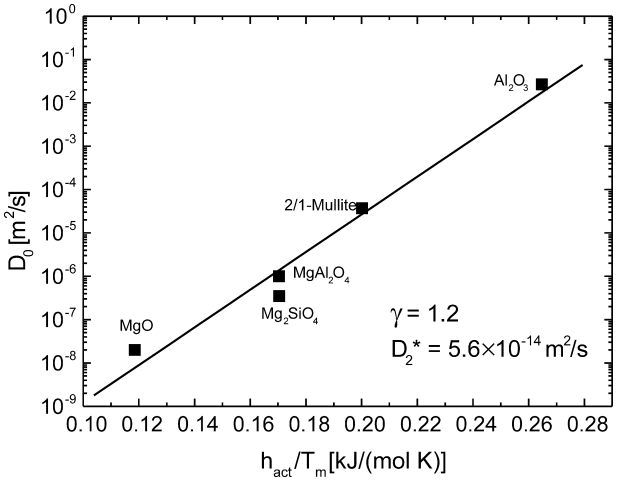

Fig. 5. The same data as in Fig. 4 plotted in a [log (D_0), h_{act}/T_m] diagram, where T_m is the melting temperature. A linear fit yields a constant slope γ and the pre-exponential factor D_2^* at zero activation enthalpy.

This means if one can find a linear correlation of diffusion data in a [log(D_0), h_{act}/T_m] diagram one can calculate a constant γ which is universal for all the different materials. Fig. 5 shows that the correlation in such a plot is much better than in Fig. 4. A linear fit in this plot results in a constant $\gamma \simeq 1.2$ which is close to one and a diffusion coefficient at zero activation enthalpy, $D_2^* = 5.6\times10^{-14}$ m^2/s. This result can be used to estimate the activation enthalpy h_{act} and the pre-exponential factor D_0 for oxygen self-diffusion in other close packed oxides, if the empirical relation between activation enthalpy and oxygen density (see Table 1) is used:

$$\begin{aligned} h_{act} &\approx 1.2\times10^{-55}\,\frac{\text{kJ}\quad \text{m}^6}{\text{mol}} \times \rho_o^2; \\ D_0 &\approx 5.6\times10^{-14}\,\frac{\text{m}^2}{\text{s}} \exp\left(\frac{h_{act}}{1.2RT_m}\right) \end{aligned} \tag{11}$$

Because of $g_{act} = h_{act} - Ts_{act}$, we find with Eq. (10) for the temperature dependence of the free enthalpy of activation in close packed oxides in the interval [T_{min}, T_{max}]:

$$\begin{aligned} &g_{act}(T) = (\gamma T_m - T)s_{act} + g_{act}^* \quad \text{with} \\ &g_{act}^* = \gamma T_m R \ln\frac{\Gamma}{D_2^*} \end{aligned} \tag{12}$$

where g_{act}^* is the hypothetical free enthalpy of activation for diffusion via a given defect at $T = \gamma\ T_m = 1.2T_m$. This experimental result indicates that g_{act}^* is correlated to the free enthalpy of activation for diffusion via this defect at the melting temperature T_m. A theoretical explanation of Eq. (12) is possible with the $cB\Omega$-model, which will be shown in the next section.

3.3. Calculation of activation parameters by the $cB\Omega$-model

Varotsos and Alexopoulos[10] have given a thermodynamically substantiated relation (called the $cB\Omega$-model) between bulk properties and the free enthalpy of activation for an individual defect:

$$g_{act}(T) = c_{act} B(T)\Omega(T) \tag{13}$$

where B is the isothermal bulk modulus, $1/B = -(\partial V/\partial p)_T/V$, and Ω is the mean volume per atom. The coefficient c_{act} is practically temperature and pressure independent and is specific to the respective defect mechanism and the crystal structure. The tracer diffusion coefficient [see Eq. (6)] is then given by:

$$D = \Gamma \exp\left(-\frac{g_{act}}{RT}\right) = \Gamma \exp\left(-\frac{c_{act} B\Omega}{RT}\right) \tag{14}$$

3.3.1. Temperature dependence of Ω

The mean volume per atom Ω above room temperature is given by:[11]

$$\Omega(T) = \Omega_r \exp\left(\int_{T_r}^{T} \alpha(T')\mathrm{d}T'\right) \quad (15)$$

where Ω_r is the volume at reference temperature (T_r, usually room temperature) and α the thermal expansion coefficient. When the thermal expansion coefficient is very small and independent of temperature over the measured temperature range the following approximation holds:

$$\Omega(T) = \Omega_r(1 + \alpha_o(T - T_r)) \quad (16)$$

For the close packed oxides in Table 1 the thermal expansion coefficient is in the order of 20×10^{-6}/K.[11] The maximum temperature for the diffusion experiments was 1950 K, so that we get for $\alpha_0(T_{max}-T_r)=0.03$. This means that the relative volume change is only in the order of 3%. Because of this small volume change we can take $\Omega \cong \Omega_r$ in the interval $[T_r, T_{max}]$.

3.3.2. Temperature dependence of the bulk modulus B

Fig. 6 shows the schematic temperature dependence of the bulk modulus.[10] At very low temperatures (region I) B decreases with temperature in a non-linear way. In regions II and III the bulk modulus B is found to decrease linearly with T. In region III the mean volume Ω starts to differ from Ω_r at room temperature. In the temperature region IV, near the melting point, B starts to decrease with T faster than linearly. This means that one can express the temperature dependence of B in the temperature regions II and III generally by $B(T)=(T^*-^T)m_B+B^*$ with $m_B=-(\partial B/\partial T)_p=$constant, where B^* is the bulk modulus at temperature T^*. Choosing $T^*=\kappa T_m$ one gets (see Fig. 6):

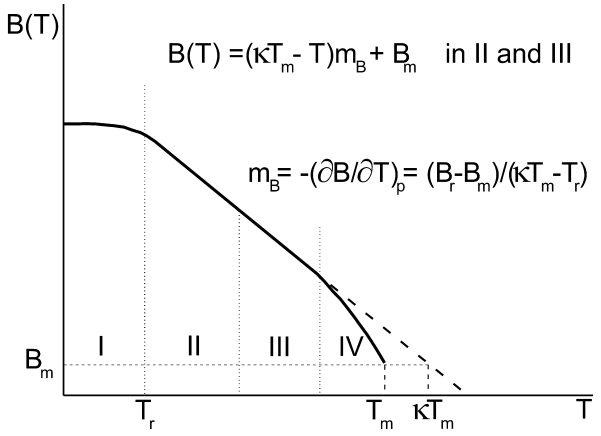

Fig. 6. Schematic temperature dependence of the bulk modulus; I: quantum region; IV: region of excessive softening.[10]

$$B(T) = (\kappa T_m - T)m_B + B_m \quad \text{with}$$
$$m_B \equiv -\left.\frac{\partial B}{\partial T}\right|_p = \frac{B_r - B_m}{\kappa T_m - T_r} \quad (17)$$

where B_r is the bulk modulus at room temperature, T_r, and B_m the bulk modulus just below the melting temperature, T_m.

3.3.3. Calculation of the activation entropy and activation enthalpy from bulk properties

From Eqs. (13) and (17) it follows for $\Omega=\Omega_r$ because of $s_{act}=-(\partial g_{act}/\partial T)_p$ for the temperature dependence of the activation enthalpy in the temperature interval $[T_{min}, T_{max}]$:

$$g_{act}(T) = c_{act}\Omega_r B(T) = (\kappa T_m - T)s_{act} + g_\kappa^* \quad \text{with} \quad (18)$$
$$g_\kappa^* \equiv c_{act}\Omega_r B_m$$

$$s_{act} = c_{act}\Omega_r m_B = c_{act}\Omega_r \frac{B_r - B_m}{\kappa T_m - T_r} \quad (19)$$

$$h_{act} = g_{act} + Ts_{act} = \kappa T_m s_{act} + g_\kappa^* \quad (20)$$

where g_κ^* is the free enthalpy of activation at $T=\kappa T_m$. This is *not* the free enthalpy of activation at the melting temperature because of:

$$g_{act}(T_m) = c_{act}\Omega(T_m)B_m = \frac{\Omega(T_m)}{\Omega_r} g_\kappa^* \quad (21)$$

The theoretical Eq. (20) is very similar to the empirical Eq. (10). This similarity suggests the following identities to be fulfilled:

$$\gamma = \kappa \quad \text{and} \quad \frac{g_\kappa^*}{T_m} = \frac{c_{act}\Omega_r B_m}{T_m} = \gamma R \ln\frac{\Gamma}{D_2^*} \quad (22)$$

In the framework of the $cB\Omega$-model we can now interpret the constant γ. It is a consequence of the linear extrapolation from low to high temperatures neglecting the fact that the bulk modulus is not linear at high temperatures (see Fig. 6). Another important conclusion from the $cB\Omega$-model is that the intersection with the h_{act}/T_m axis, g_κ^*/T_m, in a $[h_{act}/T_m, s_{act}]$ diagram is not really independent of material parameters: a perfect correlation would require the following condition to be fulfilled [compare Eq. (22)]:

$$\frac{c_{act}\Omega_r B_m}{T_m} \approx \text{constant} \quad (23)$$

4. Conclusions

The oxygen diffusion data for mullite obey both the purely empirical Reddy–Cooper transformation and a

modified compensation law. For the latter, a deeper understanding can be obtained on the basis of the so called $cB\Omega$-model by Varotsos et al.,[10] which relates the activation enthalpy for the given diffusion process directly to the melting temperature of the material. This procedure permits the estimation of activation parameters from the bulk modulus and the mean atomic volume — if they were known as a function of temperature, which is not the case for the bulk modulus of mullite.

Considering mullite as an ''alumina-doped'' sillimanite [see Eq. (1)] the resulting concentration of structural oxygen vacancies should be virtually independent of temperature. The resulting structural vacancy concentration ratio for 2/1-mullite and 3/2-mullite is 0.40/0.25 = 1.6.

This is in fair agreement with the ratio of the oxygen diffusivities in the two different mullite structures [≈2, see Eqs. (2) and (3)] and with the ratio of the oxygen vacancy concentrations introduced by the alumina doping [see Eq. (1)]. For constant oxygen activity it follows from the electroneutrality condition:

$$\left[V_{\mathrm{o}}^{\cdot\cdot}\right] = \left[Al'_{\mathrm{Si}}\right]/2 \tag{24}$$

$$\frac{\left[V_{\mathrm{o}}^{\cdot\cdot}\right]_{2/1}}{\left[V_{\mathrm{o}}^{\cdot\cdot}\right]_{3/2}} = \exp\left(-\frac{\Delta G^0_{3/2}}{9RT}\right) \tag{25}$$

where $\Delta G^0_{3/2}$ is the standard Gibbs energy of formation for the formation reaction of 3/2-mullite[12]

$$2SiO_2 + 3Al_2O_3 \Longleftrightarrow 2SiO_2 \cdot 3Al_2O_3, \quad \Delta G^0_{3/2} \tag{26}$$

For $T \cong 1700$ K and $\Delta G^0_{3/2}(1700\ \mathrm{K}) \cong -27$ kJ/mol, Eq. (25) yields a ratio of vacancy concentrations of $\left[V_{\mathrm{o}}^{\cdot\cdot}\right]_{2/1}/\left[V_{\mathrm{o}}^{\cdot\cdot}\right]_{3/2} \cong 1.24$.

The oxygen vacancy concentration ratios discussed above are identical within experimental error of both the diffusion data and the thermodynamic data and/or the error in the chemical composition of the mullite samples. This does, however, not mean that all the structural vacancies in the oxygen sublattice are mobile. If this were the case the oxygen diffusivities should be much higher, e.g. like in calcia or yttria stabilised zirconia, and the activation enthalpies should be appreciably lower ($\leqslant 1$ eV as in stabilised zirconia). Therefore, the observed high values of the activation enthalpy of diffusion (ca. 4.5 eV) must contain a formation term. It is reasonable to assume that in both limiting mullite structures the enthalpy of formation of thermal oxygen vacancies is the same. As the diffusivity data for 2/1-mullite and for 3/2-mullite differ only by a factor of about 2 in a fairly large temperature interval it is highly probable that in both cases the same fraction of thermal vacancies is excited from the reservoir of structural vacancies of the crystal. Any anisotropy must be less than the experimental error (± 30%) of the diffusivities, which is in agreement with data for other close-packed oxides.[3]

Acknowledgements

We are indebted to Dr. W. Walraffen for the production of the valuable single crystals and would like to thank E. Ebeling for very careful polishing of the samples. Financial support from Deutsche Forschungsgemeinschaft (DFG) is gratefully acknowledged.

References

1. Pleger, R. and Schneider, H., The reconstructive 2/1- to 3/2-mullite transformation in the presence of Fe_2O_3-rich glass at 1570°C. *J. Eur. Min. Soc.,* 1993, **5**, 515–521.
2. Ikuma, Y., Shimada, E., Sakano, S., Oishi, M., Yokoyama, M. and Nakagawa, Z., Oxygen self-diffusion in cylindrical single-crystal mullite. *J. Electrochem. Soc.,* 1999, **146**, 4672–4675.
3. Fielitz, P., Borchardt, G., Schmücker, M., Schneider, H., Wiedenbeck, M., Rhede, D., Weber, S. and Scherrer, S., A SIMS study of oxygen-18 tracer diffusion in 2/1-mullite single crystals. *J. Am. Ceram. Soc.*, in press.
4. Reddy, K. P. R., *Oxygen Diffusion in Close Packed Oxides*. PhD thesis, Case Western Reserve University, 1979.
5. Schneider, H., Okada, K. and Pask, J. A., *Mullite and Mullite Ceramics*. John Wiley and Sons, Chichester, 1994 p. 86.
6. Hart, S. R., Diffusion compensation in natural silicates. *Geochim. Cosmochim. Acta,* 1980, **45**, 279–291.
7. Philibert, J., *Atom Movements: Diffusion and Mass Transport in Solids*. Les Editions de Physique, Les Ulis, 1991, p. 99.
8. Zener, C. In *Imperfections in Nearly Perfect Crystals*, ed. W. Shockley. John Wiley and Sons, New York, 1992, pp. 289–314.
9. Béjina, F. and Jaoul, O., Silicon diffusion in silicate minerals. *Earth Plan. Sci. Lett.,* 1997, **153**, 229–238.
10. Varotsos, P. A. and Alexopoulos, K. D., *Thermodynamics of Point Defects and their Relation with Bulk Properties*. North-Holland, Amsterdam, 1986 pp. 163–268.
11. Ahrens, T. J., *Mineral Physics and Crystallography: A Handbook of Physical Constants*. American Geophysical Union, FL, 1995 p. 29.
12. Barin, I., *Thermochemical Data of Pure Substances*. VCH Verlagsgesellschaft, Weinheim, 1989, p. 61.